Design and Synthesis of Ionic Liquid-based MMP Inhibitors: a Simple Approach to Increase Hydrophilicity and to Develop MMPI-coated Gold Nanoparticles

Felicia D'Andrea, [a] Elisa Nuti, [a] Stefano Becherini, [+][a] Doretta Cuffaro, [+][a] Elena Husanu,[+][a] Caterina Camodeca,[a] Elena De Vita,[a] Maria Raffaella Zocchi,[b] Alessandro Poggi,[c] Cristina D'Arrigo,[d] Valentina Cappello,[e] Mauro Gemmi,[e] Susanna Nencetti,[a] Cinzia Chiappe,*[a] Armando Rossello.*[a]

[a] Dr. F. D'Andrea, Dr. S. Becherini,[+] Dr. D. Cuffaro,[+] Dr. E. Husanu,[+] Prof. E. Nuti, C. Camodeca, Dr. Elena De Vita, Dr. S. Nencetti, Prof. C. Chiappe, Prof. A. Rossello
Department of Pharmacy
University of Pisa
via Bonanno 6/33, 56126 Pisa (Italy)
E-mail: cinzia.chiappe@unipi.it, armando.rossello@unipi.it

[b] Dr. M. R. Zocchi
Division of Immunology, Transplants and Infectious Diseases,
San Raffaele Scientific Institute,
via Olgettina 60, 20132 Milan, Italy.

[c] Dr. A. Poggi
Unit of Molecular Oncology and Angiogenesis,
IRCCS AOU San Martino-IST,
Largo Rosanna Benzi 10, 16132 Genoa, Italy.

[d] Dr. C. D'Arrigo
Istituto per lo Studio delle Macromolecole, CNR,
Via De Marini 6, 16149 Genoa, Italy.

[e] Dr. V. Cappello, Dr M. Gemmi
Istituto Italiano di Tecnologia, Center for Nanotechnology Innovation@NEST,
Piazza San Silvestro 12, Pisa (Italy)

[+] These authors have contributed equally to this work

Supporting information for this article is given via a link at the end of the document.

Abstract: Selective and potent MMP-12 inhibitors endowed with improved hydrophilicity are highly sought for a potential use in the treatment of lung and cardiovascular diseases. In the present paper, we modified the structure of a nanomolar MMP-12 inhibitor (**1**) in order to incorporate an ionic liquid (IL) moiety able to improve its water solubility. Four biologically active salts (**12a-d**) were obtained by linking the sulfonamide moiety of **1** to imidazolium, pyrrolidinium, piperidinium and DABCO-based ionic liquids. The imidazolium-based bioactive salt, **12a**, was tested on human recombinant MMPs and on monocyte-derived dendritic cells showing a comparable activity with respect to **1** associated to an improved water solubility. Then, **12a** was used to prepare electrostatically stabilized MMP inhibitor-coated gold nanoparticles (AuNPs) able to selectively bind MMP-12. AuNPs were used to study subcellular localization of MMP-12 in monocyte-derived dendritic cells by TEM analysis.

Introduction

Matrix metalloproteinases (MMPs) are a family of 23 zinc-dependent endopeptidases involved in the remodelling of the extracellular matrix (ECM). They catalyse the degradation of ECM macromolecules such as the interstitial and basement membrane collagens, proteoglycans and fibronectin.[1] Many MMPs have been recognized as potential drug targets useful for the treatment of different diseases such as cancer, rheumatoid arthritis, osteoarthritis and inflammatory diseases.[2] In particular an increased expression of macrophage metalloelastase (or MMP-12) has been recognized to be involved in acute and chronic pulmonary inflammatory diseases, such as chronic obstructive pulmonary disease (COPD)[3] or asthma,[4] and in cardiovascular diseases such as aneurysms and atherosclerosis.[5] In our ongoing pursuit of MMP-12 selective inhibitors useful for the treatment of lung and cardiovascular diseases, we recently developed compound **1** (Figure 1), a carboxylate-based sulfonamide endowed with a nanomolar affinity for MMP-12. With the aim to improve the hydrophilicity and bioavailability of this very hydrophobic hit compound without decreasing its affinity for the target, we linked a β-*N*-acetyl-d-glucosamine (GlcNAc) moiety in P2' position. [6] Glycoconjugate **2** (Figure 1) maintained a nanomolar activity for MMP-12 and good selectivity over MMPs with an improved hydrophilicity (water solubility > 5 mM and cLogP = 3.15) with respect to **1**. On the basis of these results, in this study we designed and synthesized new ionic liquid-based MMP-12 inhibitors (type **3** derivatives, Figure 1) as an alternative way to improve the water solubility of our hit compound. We chose to modify the structure of compound **1** by linking its sulfonamide moiety to an ionic liquid (IL), an organic salt liquid at/or near room temperatures. [7] Through this strategy we meant to maintain the

molecular portions responsible for biological activity (i.e. the carboxylate group and the biphenylsulfonamide moiety) while introducing an IL tail in P2' position. X-ray crystallography and molecular modelling studies[8,9] had already shown that P2' could be a proper position for derivatizing sulfonamido-based MMP inhibitors and to obtain functionalized ligands with a good affinity for the target enzyme.

In the past few years ionic liquids have been exploited in the formulation of active pharmaceutical ingredients (API) because of their unique and tunable physicochemical and biological properties.[10] Many ILs bearing API in the cation or anion have been reported[11] to address problems such as low solubility, polymorphism and bioavailability of drugs. In fact, since ILs are liquid salts, turning a drug into an ionic liquid might result in a straightforward and efficient method to improve its bioavailability and to relieve the problem of polymorphs. Bioactive compounds linked to ILs could acquire the tunability of ILs and their physicochemical properties, including the ability to give spontaneous self-organized structures (micelles, vesicles) in aqueous media or through the interaction with selected supports (nanoparticles). Imidazolium-based ILs, the most investigated class of ILs, are indeed very often used as stabilizing agents in the synthesis of metal nanoparticles (NPs).[12] Possessing high dielectric constants, intrinsic ionic charge and a high polarity, the supramolecular networks that ILs give depending on cation and anion structure can form a protective shell for metal NPs, providing an electrostatic protection according to DLVO (Derjaugin-Landau-Verwey-Overbeek) theory.[13] The possibility of exploiting the IL part to obtain more complicated systems is an attractive challenge also in light of a recent document showing that AuNPs stabilized by non-covalent binders have the ability to turn off the electrons induced by radiation, opening potential applications in fields that range from radiotherapy to diagnostics.[14, 15] Recently, new ionic liquids (ILs) were synthesized and applied in synthesis of silver, gold and metal oxide nanoparticles through a simple approach.[16, 17, 18] Bearing in mind this potential application of ILs, the second aim of the present study was to prepare gold nanoparticles (AuNPs) coated with a biologically active IL able to bind MMP-12 (Figure 1).

In fact, recently the extracellular localization of MMPs boosted the research in the diagnostic field, promoting the development of modified MMP inhibitors (MMPIs) as imaging probes to visualize MMPs *in vitro* and *in vivo*. Fluorescence-labelled MMPIs were reported to be used for optical imaging [19, 20] and radiolabelled MMPIs were developed to be used for PET.[21, 22] In this context, MMPI-coated AuNPs that selectively bind a particular MMP could be of large interest for imaging purposes.

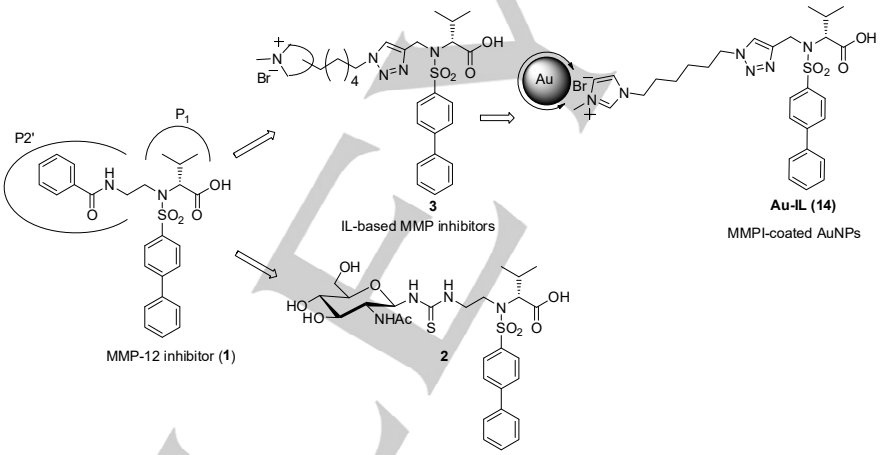

Figure 1. Chemical evolution of the new IL-based MMP inhibitors and MMPI-coated AuNPs.

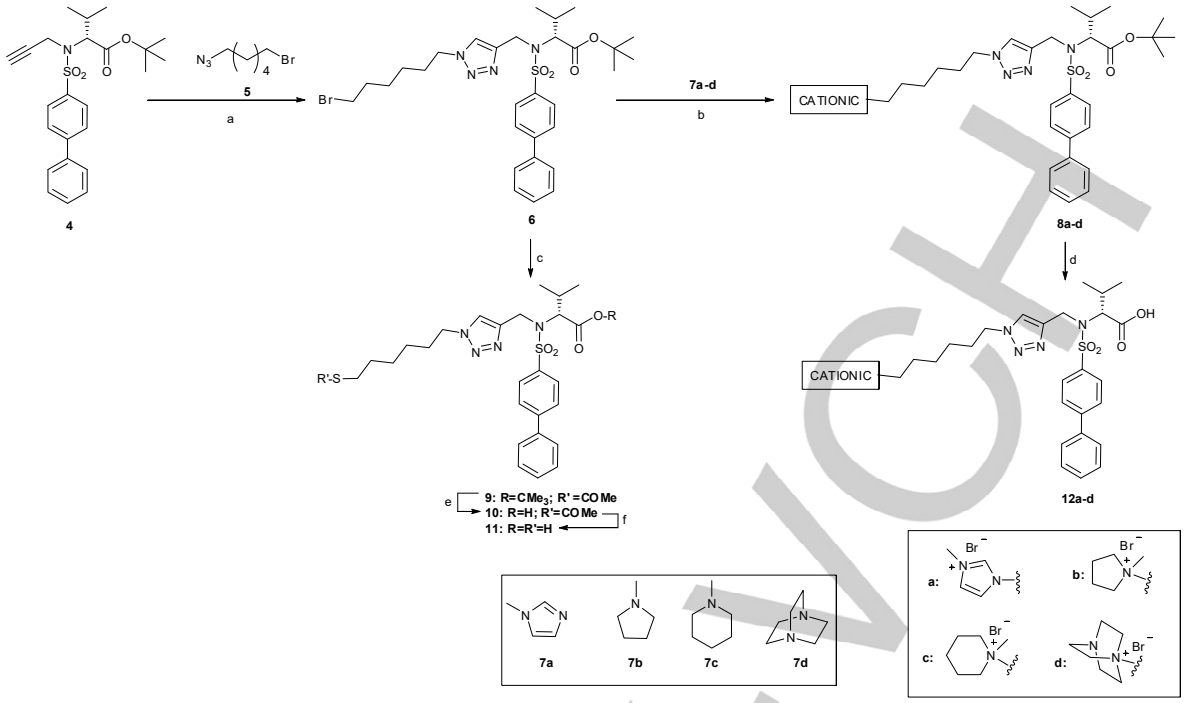

Scheme 1. Synthesis of ligands **11** and **12a-d**. Reagents and conditions: (a) $CuSO_4 \cdot 5H_2O$, sodium ascorbate, 1:4 H_2O-DMF, 80 °C, 1 h (87%); (b) CH_3CN, 80 °C, 3-10 days (91% for **8a**, 77% for **8b** and 78% for **8c**) or EtOAc, rt, 3 days (82% for **8d**); (c) potassium thioacetate, DMF, 120 °C, 2.5 h (98%); (d) 48% aq. HBr, H_2O rt, 8-12 h (92% for **12a**; 94% for **12b**; 93% for **12c** and 99% for **12d**); (e) TFA, CH_2Cl_2, rt, 8 h (98%); (f) NH_3-MeOH 3.5 N, rt, 4 h (89%).

Currently, AuNPs represent an emerging new class of probes for cellular imaging suitable for protein visualization through electron microscopy (EM). AuNPs are particularly interesting since they are endowed with high chemical stability, low toxicity to mammalian cells and they are easily modifiable with the molecules of interest. [23]

In the present study, IL-based MMP inhibitors **12a-d** (Scheme 1) and MMPI-coated **Au-IL (14)** (Figure 1) were synthesized, characterized and tested on human recombinant MMPs to prove their activity *in vitro*. The sulfonamide moiety of **1** was linked to imidazolium, pyrrolidinium, piperidinium and DABCO-based ionic liquids on the basis of their wide use in literature. [7, 11] Then, the biological activity of the imidazolium-based bioactive salt, **12a**, was tested on monocyte-derived dendritic cells (DC) in comparison with the parent compound **1.** The activity of the electrostatically stabilized **Au-IL (14)**, obtained using **12a**, on recombinant MMPs was compared to the one of **Au-S (13)** (Scheme 2) obtained using the thiol **11**, through the conventional Au-S bond. Finally, these AuNPs were used to visualize the subcellular localization of MMP-12 in DC by TEM analysis.

Results and Discussion

Chemistry

The synthesis of IL-based MMP inhibitors **12a-d** and their analogue thiol **11** is described in Scheme 1. The known alkynyl derivative **4**[6] and 1-azido-6-bromohexane **5** [24] were prepared in according to published procedures. The azide **5** was conjugated to the alkyne **4** by copper-catalysed azide-alkyne cycloaddition (CuAAC) according to reported conditions. [25, 26] The reaction was performed in a mixture DMF-H_2O (4:1) with copper(II) sulphate and sodium ascorbate as catalytic system, at room temperature for 1 h. The purification by flash chromatography of crude products yielded pure **6** (87%) with complete regiospecificity. NMR analysis (^1H, ^{13}C and 2D NMR experiments) of the isolated product showed indeed the exclusive formation of the 1,4-disubstituted 1,2,3-triazole **6**, which was identified on the basis of the large Δ (δC4-δC5) values (about 20 ppm) observed by ^{13}C NMR spectroscopy for the cycloadducts.

The bromine derivative **6** was a suitable precursor for the preparation of the ionic salts **8a-d** through a S_N2 type reaction using opportune amines (*N*-methyl-imidazole **7a**; *N*-methyl-pyrrolidine **7b**; *N*-methyl-piperidine **7b**; 1,4-diazabicyclo[2.2.2]octane **7d**). In particular, the preparations of **8a-c** were carried out in dry CH_3CN at 80 °C (3-10 days) while the synthesis of **8d** was conducted in dry EtOAc at room temperature (3 days). The purification by trituration of the crude products with Et_2O afforded pure **8a-d** in high yield (91-77%). The thiol derivative **11** was obtained from the thioester derivative **9** (Scheme 1) by treatment of **6** with potassium thioacetate in dry DMF at 120 °C. The purification by flash chromatography on silica gel afforded thioester pure **9** in excellent yield (98%).

The treatment of **9** with CF_3COOH gave the corresponding carboxylic acid **10** (98%) after chromatography over silica gel of crude product. The removal of the *tert*-butyl group in **8a-d** by treatment with commercial 48% aq. HBr in H_2O gave the corresponding carboxylic acids **12a-d** (92-99%), after trituration with Et_2O of crude products. Finally, the de-*O*-acetylation of **10** by treatment with NH_3-MeOH 3.5N afforded the deprotected thiol derivative **11** in good yields (89%), after trituration of crude product with Et_2O. The structure of all compounds were confirmed by ^1H, ^{13}C and 2D NMR experiments.

Traditional Au nanoparticles **Au-S (13)** were prepared as reported in Scheme 2 following a reported procedure [27] in heterogeneous

phase ($CHCl_3$-H_2O), using ALIQUAT 336 as phase transfer agent, the thiol derivative **11**, and a solution of tetrachloroauric acid ($HAuCl_4$) and sodium borohydride ($NaBH_4$) as reducing agent (see experimental section). The purification of crude mixture by dialysis and elimination of solvent under reduced pressure yielded **Au-S (13)** as a dark brown syrup.

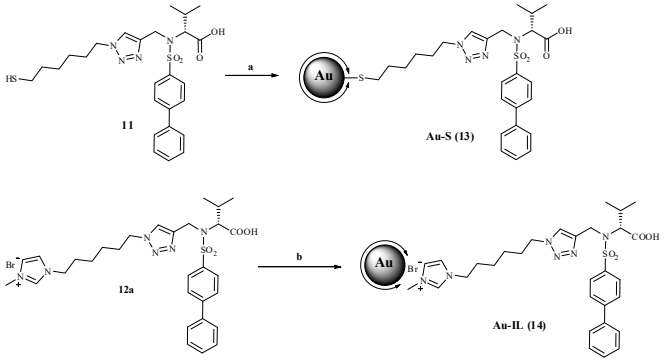

Scheme 2. Synthesis of **Au-S (13)** and **Au-IL (14)**. Reagents and conditions: (a) 1) $CHCl_3$, ALIQUAT 336, $HAuCl_4$ 2.5 x 10^{-3} M; 2) $NaBH_4$ 0.1 M. (b) 0.1:1 CH_3OH-H_2O, $HAuCl_4$ 2.5 x 10^{-3} M, $NaBH_4$ 0.1 M.

The UV-Vis spectrum of **Au-S (13)** was characterized by an intense absorption band at 268 nm, corresponding to the MMPI unit, and by a very weak band at 518 nm attributable to the surface plasmon resonance (SPR) of AuNPs (Figure 2).

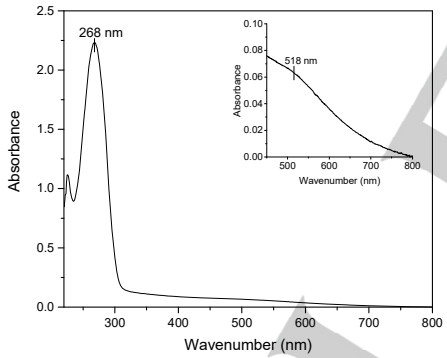

Figure 2. UV-vis spectrum showing the characteristic absorption band of biphenyl chromophore; in the inset, magnified LSPR band of **Au-S (13).**

Although, the low intensity of the SPR band could suggest AuNPs agglomeration phenomenon, in our case the brown solution is still stable after 5 months and, therefore, the low intensity is more probably due to the very small size of the synthesized **Au-S (13)** that have the absorption in IR domain. [28] This hypothesis found his experimental support in the TEM measurements (Figure 3).

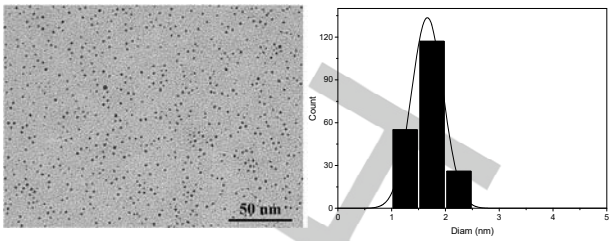

Figure 3. (left) TEM brightfield image of the **Au-S (13)**; (right) nanoparticles' diameter distribution.

The average diameter and the standard deviation obtained from the measurements of 200 nanoparticles **Au-S (13)**, resulted 1.5 ± 0.2 nm. Furthermore, it is noteworthy that UV-Vis measurements using a calibration curve (see supporting information, Figure S1 and S2) show that 53% of the charged biologically active compound (MMPI) remains bound to the **Au-S (13)**. [29]

The electrostatically stabilized AuNPs **Au-IL (14)** were instead synthesized starting from the ionic ligand **12a** (Scheme 2). In particular, they were prepared through a single-step process by reducing a solution of $HAuCl_4$ with $NaBH_4$, in the presence of ligand **12a** in 0.1:1 MeOH-H_2O (see experimental section), followed by purification through centrifugal filtration with filter Millipore Amicon 14 kDa to remove residual small molecules. After centrifugation, **Au-IL (14)** were re-dispersed in water. The resulting solution, which did not show any evidence of aggregation, strongly suggested that the ionic ligand was able to make the resulting nanoparticles coated with bioactive molecules not only very soluble in the aqueous environment, in contrast with the starting MMPI, but also not prone to interact reciprocally. It is also to remark that the colour of the solution containing these AuNPs, synthesized using the imidazolium-based bioactive salt **12a**, immediately after purification appeared almost violet and the UV-Vis spectrum was characterized by the SPR maximum at 538 nm (Figure 4a).

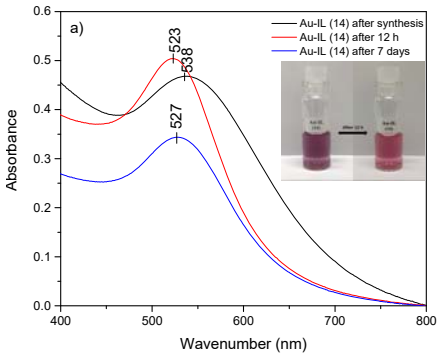

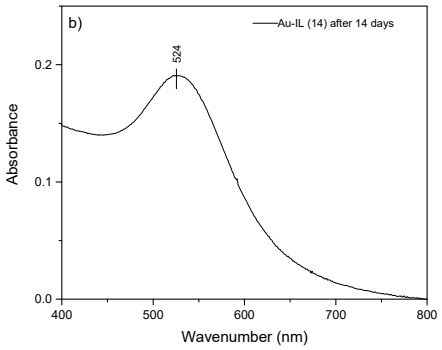

Figure 4. Stability with time of AuNPs **Au-IL (14)**; (a) readings in 1 cm quartz cuvette: in the inset, the change of colour from violet to pink; (b) UV-vis spectrum after 14 days in 1 mm quartz cuvette.

However, after two days the colour of the solution changed into ruby red and the SPR band blue shifted to 523 nm. This behaviour, i.e. the slow blue shift of the SPR band, although not usual for AuNPs, has been already reported for NPs stabilized with non-covalent binding, such as electrostatic interactions. For example, it has been observed in the case of AgNPs capped with Rhodamine 6G and attributed to the close packing of the dye molecules on the charged particle surface that determines a time requiring tuning of the coating molecules on particles surface. [30] A phenomenon of this type could occur also in our case due to the presence in the imidazolium salt **12a** of the biphenyl system of the MMPI that absorbs also in this region and has steric requirements.

TEM measurements carried out on 200 nanoparticles allowed to evaluate for **Au-IL (14)** an average diameter of 3.0 ± 0.5 nm (Figure 5).

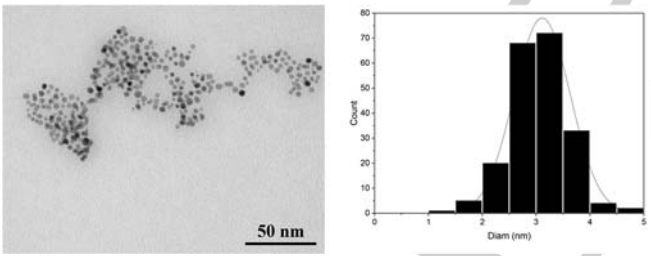

Figure 5. (left) TEM brightfield image of **Au-IL (14);** (right) nanoparticles' diameter distribution.

As expected, the use of an ionic ligand (**12a** vs **11**) for the preparation of AuNPs is important in terms of size control. Nonetheless, the stability of the colloidal solutions (experiments were carried out in triplicate) were monitored during the time (Figure 4a and 4b). Although, after the initial shift of the SPR band the absorption maximum remained practically unchanged, a progressive slow decrease of the same absorption band, attributable to the agglomeration of the AuNPs, was evidenced (see supporting information UV-Vis after 60 days, Figure S4).

Finally, through a UV-Vis measurements (see supporting information, Figure S1 and S3) it was evaluated that 47% of the charged imidazolium derivative **12a** remained adsorbed on nanoparticles **Au-IL (14)**.

AuNPs stability studies.

Since the electrostatically stabilized MMPI-coated AuNPs **Au-IL (14)** should be tested on recombinant enzymes, their stability in buffer solution was preliminary checked using a fluorometric assay buffer (FAB), at pH 7.5. In particular, a known quantity of **Au-IL (14)** was added to FAB and the absorption at 526 nm was monitored during the time showing that the solution was stable under these conditions for few days (Table 1).

Furthermore, the storage conditions were investigated splitting the same sample into two aliquots: one was stored in the dark the other in a lighted area. As reported in Table 1, no significant differences were registered in the UV-Vis spectrum.

Table 1. λ_{max} of SPR and biphenyl unit for **Au-IL (14)** in different conditions.

AuNPs	Conditions	λ_{SPR}	λ_{max} biphenyl
Au-IL (14)	--	525 nm	268 nm
Au-IL (14)	After 12 h dark	524 nm	268 nm
Au-IL (14)	After 12 h light	527 nm	268 nm
Au-IL (14)	FAB pH 7.5	526 nm	268 nm

The influence of the cationic moiety on AuNPs stability was also investigated. The *N*-methylimidazolium cation was indeed replaced with alicyclic quaternary ammonium cations such as piperidinium (Pip), pyrrolidinium (Pyrr) or the bicyclic system arising from monoalkylation of 1,4-diazabicyclo [2.2.2] octane (DABCO). In order to favour the comparison, the chemical structure of the linker, the MMPI and the anion were not modified. It is noteworthy that attempts to prepare AuNPs using the ionic ligands **12b-d** (Scheme 1), in accordance with the procedure described above for AuNPs **14**, failed (see Supporting Information, Figure S5 and S6). All the three salts based on aliphatic onium cations were unable to give stable Au colloidal solutions, since the agglomeration of the nanoparticles occurred during the synthesis. These data suggest that the aromatic imidazolium ring, characterized by a planar structure and a delocalized positive charge, is more incline to give self-assembled and well organized nanostructures on the metal surface playing therefore an important role in Au colloidal solution stabilization. [31]

MMPs inhibition.

The inhibitory activity of all the new potential MMPIs containing the biologically active sulfonamide moiety of **1**, i.e. the IL-based MMPIs **12a-d**, the thiol derivative **11** and the MMPI-coated AuNPs **Au-S (13)** and **Au-IL (14)**, were tested on human recombinant MMPs by a fluorometric assay, [32] using the previously reported **1** as reference compound. Activity was evaluated against MMP-12, as target enzyme, and against MMP-2 and MMP-9 to assess the selectivity of the new compounds. The activity of **1** towards these enzymes was already demonstrated. [6] Results are reported in Table 2 as IC_{50} values (nM).

Table 2. Inhibitory activity (IC_{50} nM values)[a] of **11**, **12a-d**, **Au-S (13)**, **Au-IL (14)** and the reference compound **1**.

Compound	MMP-2	MMP-9	MMP-12
11	2300±200	5700±560	214±23

12a	200±11	2300±280	60±4.2
12b	240±28	2850±300	72±9
12c	200±29	2000±190	60±7
12d	330±29	3700±380	88±7.3
Au-S (13)	2400±120	6800±560	210±29
Au-IL (14)	290±35	2000±110	100±7
1[6]	170±13	510±44	35±2.3

[a] Assays were run in triplicate. The final values given here are the mean ± SD of three independent experiments.

Overall, all new compounds and nanosystems showed a higher affinity for MMP-12 than for MMP-2 and MMP-9. More in detail, whereas the replacement of the *N*-ethylene-benzamide group in P2' of **1** with a 1,2,3-triazole thioalkyl chain as in compound **11** led to a decrease of activity towards all tested enzymes, the introduction of a cationic head on the linear alkyl chain restored the inhibitory activity against the target MMP-12 (compounds **12a-d**). Among the four biologically active ILs, **12a-d**, the best selectivity results were achieved by the DABCO derivative **12d**, which showed a IC_{50}= 88 nM on MMP-12 and a 42-fold selectivity over MMP-9, while the most active on MMP-12 were the piperidinium derivative **12c** and the imidazolium derivative **12a** (both with an IC_{50} = 60 nM). However, the small difference of activity characterizing the IL-based MMPIs suggests a positioning of the ionic portion of the molecule outside the active site of MMP-12, in the water-exposed region of the catalytic domain.

As initially hypothesized during the design of these ligands, IL-based compounds **12a-d** are characterized by a significantly increased hydrophilicity with respect to **1** and to the thiol derivative **11**, calculated as the partition coefficient between octanol and water, logP (o/w) reported in Table 3.

Table 3. clogP[a] of **11**, **12a-d** and the reference compound **1**.

Compound	clog*P*	Compound	clog*P*
1	5.89	**12b**	1.30
11	5.45	**12c**	1.86
12a	0.95	**12d**	1.12

[a] ACD laboratory software version 14.0 (Advanced Chemistry Development, Inc. Toronto, Canada).

On the basis of these calculations, the most lipophilic inhibitors, **1** and **11,** have a clogP > 5 while the new IL-based MMPIs have clogP values ranging between 0.95 for **12a** (the most hydrophilic of the four) and 1.86 for **12c**.

As regards the affinity for MMP-12 showed by MMPI-coated AuNPs, **Au-S (13)** and **Au-IL (14)**, they both maintained the activity and selectivity profile of the corresponding MMPI ligands (**11** and **12a**, respectively). In particular, the ionic **Au-IL (14)**, showed an IC_{50}= 100 nM on MMP-12 and a 20-fold selectivity over MMP-9, thus maintaining a good binding with the target enzyme. The small decrease of activity shown by AuNPs with respect to the hit compound **1**, could be correlated with the length of the linker introduced in P2' position, probably not sufficient to avoid interference of this type of multivalent NPs with the catalytic domain of several enzyme units.

At this point, the biological activity of the imidazolium-based bioactive salt, **12a**, was evaluated in an appropriate cell model in comparison with **1**.

Binding and biological activity of 12a on monocyte-derived DC.

To compare the biological activity of the IL-based inhibitor **12a** and its parental compound **1**, Matrigel transmigration by DC obtained from four different donors was evaluated, as it is known that DC use MMP-12 to degrade and invade extracellular matrix.[33] The assay was performed in the absence or presence of 10 μM **12a** or compound **1**. Figure 6 shows that both MMP-12 inhibitors could reduce by 20-30% DC migration, although variability in drug response among donors (042 and 044 being high responders, while 039 and 044 behaved as low responders, Figure 6A) has been observed (SD in Figure 6B).

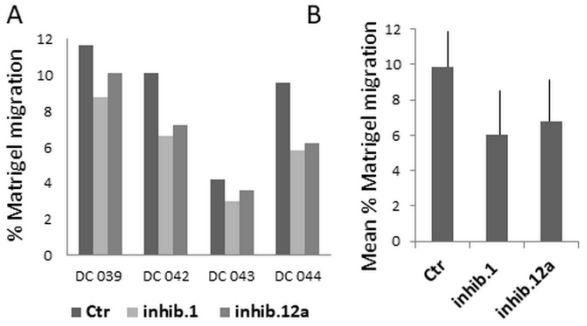

Figure 6. Effect of **12a** on Matrigel transmigration by DC in comparison with **1**. DC ($5x10^5$) were pre-incubated for 1 h at 37 °C with compound **12a** or **1** at 10 μM, then added to Matrigel-coated transwell. After 24 h at 37 °C, cells recovered from the lower chamber were counted with MACSQuant Analyzer and results plotted as percentage migrated cells vs input (A) or mean percentage migrated cells vs input (B).

Binding to MMP-12 in this cell model was checked by using a FITC-labeled derivative of **1**, **EDV2** (Supporting Information). The binding of this fluorescent probe was first assayed by FACS analysis upon incubation, at 10 to 1 μM concentrations, with DC obtained from 4 different donors. As shown in Figure 7, **EDV2** reacted with DC at 1 or 2 h (Figure 7A, left and central panels), and the staining was maintained up to 24 h (Figure 7A, right panel). Titration showed that the best binding is detected at 10 μM concentration after 24 h (Figure 7B). Confocal microscopy in Figure 7C, shows the staining of DC with 10 μM **EDV2** and 1 μM Syto62 to define nuclei. **EDV2** staining shows a partially cytoplasmic and nuclear distribution, with areas of co-localization (C: light blue dots with white arrows in c and white arrows in d and e). These results are consistent with recent literature data highlighting that MMP-12 can be located intra- and extracellularly.[34]

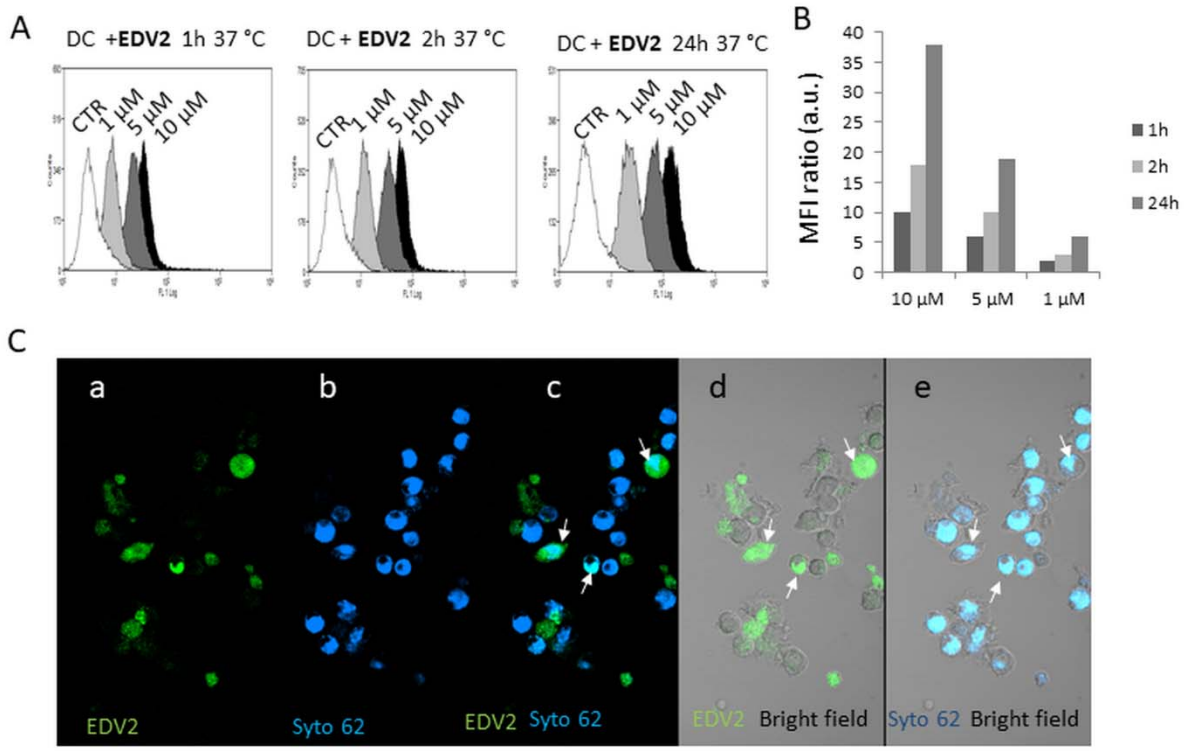

Figure 7. Staining of fluorescent probe **EDV2** in DC. A,B: DC were pre-incubated with **EDV2** (dark grey: 10 µM, grey: 5 µM, light grey: 1 µM), reactivity of FITC IgG as negative control (CTR) for 1 h (left panel), 2 h (central panel) or o.n. (24 h, right panel). Samples were then washed and analyzed on a CyAn ADP Analyzer. Results are shown as mean fluorescence intensity (MFI, arbitrary units, a.u.) vs number of cells (A) or MFI ratio vs negative control (B). Negative control (white histograms): unrelated FITC-conjugated Ig. C: DC treated with 10 µM **EDV2** and 1 µM Syto62 for 1 h at 37 °C were washed and seeded onto a glass slide and analyzed by confocal microscopy under a FV500 (Olympus Europe) with PlanApo 40x NA1.00 oil objectives and data analyzed with FluoView 4.3b software (Olympus). Images were taken in sequence mode and shown in pseudocolor.

TEM analysis of Au-IL (14) and Au-S (13) uptake in monocytes.

TEM analysis of cultured monocytes untreated (Figure 8A, CTRL), or exposed for 24 h to the gold nanoprobes **Au-IL (14)** (Figure 8B, C), or **Au-S (13)** (Figure 8D, E, F) showed a common repertoire of evidences including single-membrane or double layered vesicular structures, interspersed electron-dense particles, referable bona fide to endosomes, lysosome-like dense bodies and condensed lipids of different size and shape. Empty autophagic vesicles appeared as electron-translucent structures. Microvesicles in sub-micron scale (200-500 nm) of the endolysosomal compartment (indicated by arrows) enveloped **Au-IL (14)** and **Au-S (13)** aggregates.[35, 36] One Au aggregate was detectable in a membrane protrusion (D), magnificated in E), indicative of membrane dynamics involved in Au particle uptake or extrusion.

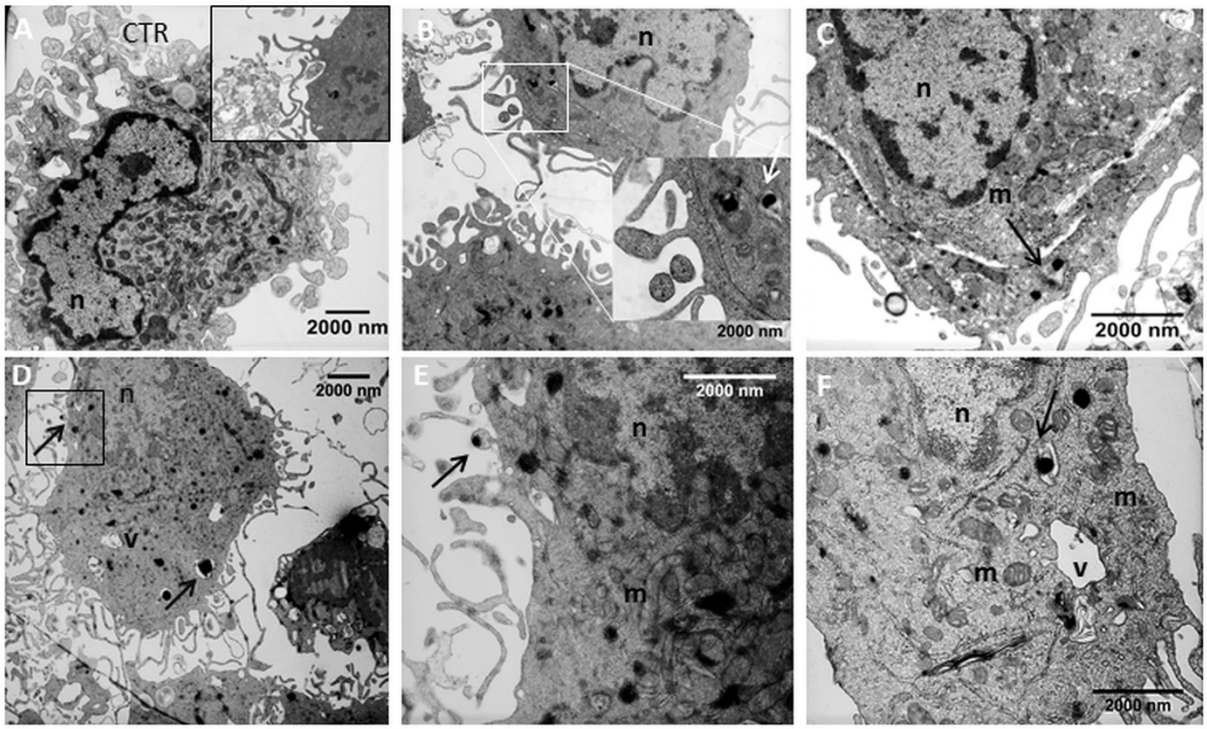

Figure 8. Localization of gold-conjugates of MMPs inhibitors by TEM analysis. Monocytes untreated (CTRL) (A), or exposed for 24 h to the gold nanoprobe **Au-IL (14)** (B, C), or **Au-S (13)** (D, E, F). AuNPs were detectable as aggregates wrapped by microvesicles of the endolysosomal compartment (indicated by arrows). The vesicles size is in sub-micron scale (200-500 nm). The inset in A) represents negative controls incubated with unconjugated gold nanoparticles. A blebbing structure (D), enlarged in E), is indicative of exo- and endocytosis. m: mitochondria; n: nuclei; v: autophagic vesicles or vacuoles.

Conclusions

In the present study, IL-based MMP-12 inhibitors have been synthesized for the first time as an alternative way to improve the hydrophilicity and bioavailability of a previously developed hit compound **1**, a sulfonamido-based carboxylate with nanomolar activity towards MMP-12. Four biologically active salts (**12a-d**) were straightforwardly obtained by linking the sulfonamide moiety of **1** to imidazolium, pyrrolidinium, piperidinium and DABCO-based ionic liquids. Furthermore, the imidazolium-based bioactive salt, **12a**, was used to prepare electrostatically stabilized MMPI-coated gold nanoparticles **Au-IL (14)**, that selectively bind MMP-12. Electrostatically stabilized AuNPs were characterized by transmission electron microscopy (TEM) and UV-Vis spectroscopy**.** Then, IL-based MMPI **12a-d** and MMPI-coated **Au-IL (14)**, were tested on human recombinant MMPs to prove their activity *in vitro*. The activity of the electrostatically stabilized **Au-IL (14)**, was compared to the one of **Au-S (13)**, obtained through the conventional Au-S bond.

The biological results showed that:

1. IL-based MMPIs **12a-d** are characterized by a significantly increased hydrophilicity (calculated as clogP) with respect to **1**, associated to a comparable activity towards the target enzyme MMP-12;
2. electrostatically stabilized AuNPs **Au-IL (14)**, have an average diameter of 3.0 ± 0.5 nm, are soluble in water and are stable in buffer solution at pH 7.5 for a few days;
3. **Au-IL (14)**, have an IC_{50}= 100 nM on MMP-12 and a 20-fold selectivity over MMP-9, thus maintaining a good binding with the target enzyme. The small decrease of activity with respect to the hit compound **1**, could be due to the non-optimized length of the linker introduced in P2' position.

Finally, the biological activity of **12a** was tested on monocyte-derived DC in comparison with the parent compound **1**. Both compounds showed a similar activity, inhibiting by 20-30% DC migration trough Matrigel. A FITC-labelled derivative of **1**, **EDV2**, was synthesized and used to visualize the binding to MMP-12 in DC. EDV2 staining showed a partially cytoplasmic and in part nuclear distribution of MMP-12, with areas of co-localization.

In conclusion, innovative IL-based MMP-12 inhibitors have been synthesized for the first time and could represent an effective way to improve the hydrophilicity and bioavailability of MMP inhibitors in general. Of course, to fully appreciate the effect of the improved bioavailability an in vivo assay would be necessary.

Moreover, electrostatically stabilized AuNPs coated with a biologically active salt able to bind MMP-12 have been successfully obtained and might be used as an innovative bioimaging probe for cell studies. An example of subcellular localization study was conducted by TEM analysis using the gold nanoprobes to stain MMP-12 in monocyte-derived DC.

Experimental Section

Materials and methods. Melting points were determined with a Kofler hot-stage apparatus and are uncorrected. ^{1}H NMR spectra were recorded in appropriate solvents with a Bruker Avance II operating at 250.13 MHz. ^{13}C NMR spectra were recorded with the spectrometer operating at 62.9 MHz. The assignments were made, when possible, with the aid of DEPT-135, HSQC and COSY experiments. The first order proton chemical shifts δ are referenced to either residual CD_3CN (δ_H 1.94, δ_C 1.28) or residual CD_3OD

(δ_H 3.31, δ_C 49.0) and J-values are given in Hz. All reactions were followed by TLC on Kieselgel 60 F_{254} with detection by UV light and/or with ethanolic 10% phosphomolybdic or sulfuric acid, and heating. Kieselgel 60 (Merck, 230-400 mesh) was used for flash chromatography. Some of flash chromatography were conducted by the automated system Isolera Four SV™ (Biotage®), equipped with UV detector with variable wavelength (200-400 nm). All reactions involving air- or moisture-sensitive reagents were performed under argon atmosphere using anhydrous solvents. Anhydrous dimethylformamide (DMF), dichloromethane (CH_2Cl_2) and acetonitrile (CH_3CN) were purchased from Sigma-Aldrich. Other dried solvents were obtained by distillation according to standard procedure[37] and stored over 4Å molecular sieves activated at least 12 h at 200 °C. $MgSO_4$ was used as the drying agent for solutions.

Tetrachloroauric acid ($HAuCl_4$) was purchased from Cabro SpA (Arezzo, Italy). All the equipment used for the preparation of gold nanoparticles were previously washed with an aqueous solution of HNO_3 10% and left for 24 h at 120 °C. The water used for the synthesis of the gold nanoparticles was MilliQ water (18 MΩ/cm).

Filters Millipore Amicon® Ultra-4 10 kDa (Sigma-Aldrich) were used as received. The dialysis tubed 14 kDa (Sigma-Aldrich) was subjected to washing with H_2O (3 h), treated with an aqueous solution of Na_2SO_3 0.3% (w/v) at 80 °C (1 minute), washing with H_2O at 60 °C (2 minutes), acidification with H_2SO_4 0.2% (v/v) and, finally, washing with warm H_2O to completely remove the acid. The centrifugation of gold nanoparticle was performed on a centrifuge REMI R-8D operating at 6000 RMP max.

UV-visible spectra were obtained in $CHCl_3$ or H_2O on an Agilent Cary 300 UV-Vis instrument, with a fixed slit width of 1 nm using 1 cm and 1 mm quartz cuvettes.

Transmission Electron Microscopy (TEM) was performed on a Zeiss Libra 120 plus operating at 120 kV and equipped with an in column omega filter for energy filtered imaging. The samples were prepared by deposition of Au nanoparticles suspended and sonicated in ethanol on a 300 mesh carbon coated copper grid. Compounds (*R*)-*tert*-Butyl 3-methyl-2-(*N*-(prop-2-ynyl)biphenyl-4-ylsulfonamido)butanoate (**4**)[6] and 1-azido-6-bromohexane (**5**)[24] were prepared according to the reported procedures.

Preparation of 1,2,3-triazole derivative (6). A solution of the azide **5**[24] (331 mg, 1.60 mmol) in a mixture of DMF-H_2O 4:1 (30 mL) was treated with $CuSO_4{\cdot}5H_2O$ (544 mg, 2.18 mmol), sodium ascorbate (867 mg, 4.37 mmol) and the know alkyne **4**[6] (624 mg, 1.45 mmol). The mixture was stirred at 80 °C until the TLC analysis (n-hexane/EtOAc 6:4) revealed the disappearance of the starting material (R_f = 0.62) and the formation of a major product at R_f = 0.33. The solvent was evaporated under reduced pressure and the residue was partitioned between saturated NH_4Cl solution (15 mL) and CH_2Cl_2 (15 mL), the organic phase was separated and the aqueous layer extracted with CH_2Cl_2 (3 × 15 mL). The collected organic phases were dried, filtered and concentrated under reduced pressure. The flash chromatographic purification on silica gel (6:4 hexane-EtOAc) of the crude residue (2.94 g) afforded triazole-linked derivative pure **6** (802 mg, 87% yield) as pale yellow oil; R_f = 0.33 (n-hexane/EtOAc 6:4); ^{1}H NMR (250.13 MHz, CD_3CN) δ = 7.86 (m, 2H, 2 × Ar-*H*), 7.83-7.75 (m, 3H, 2 × Ar-*H*, C*H*-triazole), 7.68-7.59 (m, 2H, 2 × Ar-*H*), 7.54-7.40 (m, 3H, 3 × Ar-H), 4.85, 4.64 (AB system, 2H, J_{AB} = 16.6 Hz, CH_2NSO$_2$), 4.29 (t, 2H, J_{vic} = 7.1 Hz, CH_2N), 3.92 (d, 1H, J_{vic} = 10.5 Hz, C*H*NSO$_2$), 3.41 (t, 2H, J_{vic} = 6.8 Hz, CH_2Br), 2.20 (m, 1H, *CH*Me$_2$), 1.83-1.73 (m, 4H, CH_2CH$_2$Br, CH_2CH$_2$N), 1.38 [m, 2H, *CH*$_2$(CH$_2$)$_2$N], 1.25 [m, 2H, *CH*$_2$(CH$_2$)$_2$Br], 1.23 (s, 9H, C*Me*$_3$), 0.89 (d, 3H, J_{vic} = 6.5 Hz, CH*Me*$_2$), 0.71 (d, 3H, J_{vic} = 6.5 Hz, CH*Me*$_2$); ^{13}C NMR (62.9 MHz, CD_3CN) δ =170.5 (C=O), 146.1 (*C*-triazole), 145.8 (Ar-*C*-SO$_2$), 140.0, 139.9 (2 × Ar-*C*), 130.0-128.1 (Ar-*C*H), 125.0 (*C*H-triazole), 82.8 (Me$_3$*C*), 67.6 (*C*HNSO$_2$), 50.5 (*C*H$_2$N), 40.9 (*C*H$_2$NSO$_2$), 35.1 (*C*H$_2$Br), 33.2 (*C*H$_2$CH$_2$Br), 30.7 (*C*H$_2$CH$_2$N), 29.6 (*CH*Me$_2$), 28.0 [*C*H$_2$(CH$_2$)$_2$N], 26.1 [*C*H$_2$(CH$_2$)$_2$Br], 27.8 (*Me*$_3$C), 19.9, 19.3 (*Me*$_2$CH); Anal. calcd for $C_{30}H_{41}BrN_4O_4S$: C 56.87, H 6.52, found: C 56.85, H 6.50.

General Procedure for preparation of 8a-c. To a solution of the 1,2,3-triazole derivative **6** (1 mmol, 1 eq) in dry MeCN or EtOAc (1.0 mL) was added a solution 1:10 v/v of the appropriate amines **7a**, **7b**, **7c** or **7d** (1 mmol, 1 eq) in dry CH_3CN or EtOAc. The mixture was stirred either at 80 °C or room temperature until the starting material was disappeared (3-10 days, TLC). The solvent was removed under reduced pressure and the purification of crude product by trituration with Et_2O afforded pure salt derivatives **8a**, **8b, 8c** and **8d.**

Imidazolium salt *tert*-butyl ester (8a). The title compound was prepared in dry MeCN (55 μL) from *N*-methyl-imidazole (**7a**) (0.055 mmol, 1 eq) and 1,2,3-triazole derivative **6** (35.0 mg, 0.055 mmol, 1 eq) in accordance with the general procedure. The reaction was performed at 80 °C and stopped (TLC, n-hexane/EtOAc 1:1) after 3 days. Purification of the crude product (37 mg) by trituration with Et_2O afforded pure imidazolium salt derivative **8a** (35.8 mg, 91% yield), as a very hygroscopic white solid; ^{1}H NMR (250.13 MHz, $CDCl_3$) δ = 10.2 (s, 1H, Im-*H*$_2$), 7.83-7.76 (m, 3H, 2 × Ar-*H*, C*H*-triazole), 7.63 (m, 2H, 2 × Ar-*H*), 7.50-7.46 (m, 2H, 2 × Ar-*H*), 7.41-7.21 (m, 5H, 3 × Ar-*H*, Im-*H*$_4$, Im-*H*$_5$), 4.91, 4.55 (AB system, 2H, J_{AB} = 16.7 Hz, CH_2NSO$_2$), 4.28 (m, 4H, 2×CH_2N), 4.01 (s, 3H, CH_3N), 3.89 (d, 1H, J_{vic} = 10.3 Hz, C*H*NSO$_2$), 2.19 (m, 1H, *CH*Me$_2$), 1.82 (m, 4H, 2 × CH_2CH$_2$N), 1.27 (m, 4H, CH_2CH_2), 1.12 (s, 9H, C*Me*$_3$), 0.82 (d, 3H, J_{vic} = 6.5 Hz, CH*Me*$_2$), 0.64 (d, 3H, J_{vic} = 6.5 Hz, CH*Me*$_2$); ^{13}C NMR (62.9 MHz, $CDCl_3$) δ = 169.4 (C=O), 145.6, 145.5 (Ar-*C*-SO$_2$, *C*-triazole), 139.1, 138.1 (2 × Ar-*C*), 137.3 (Im-*C*$_2$), 130.0-127.1 (Ar-*C*H), 124.3 (*C*H-triazole), 123.4, 122.0 (Im-*C*$_4$, Im-*C*$_5$), 82.0 (Me$_3$*C*O), 66.5 (*CH*NSO$_2$), 49.7, 49.5 (2 × *C*H$_2$N), 40.3 (*C*H$_2$NSO$_2$), 36.6 (*C*H$_3$N), 29.8, 29.6 (2 × *C*H$_2$CH$_2$N), 28.9 (*CH*Me$_2$), 27.6 (C*Me*$_3$), 25.3, 25.0 (*C*H$_2$CH$_2$), 19.7, 18.9 (CH*Me*$_2$). Anal. calcd for $C_{34}H_{47}BrN_6O_4S$: C 57.05, H 6.62, M, found: C 57.03, H 6.64.

Pyrrolidinium salt *tert*-butyl ester (8b). The title compound was prepared in dry MeCN (3.0 mL) from *N*-methyl-pyrrolidine (**7b**) (8.5 mg, 0.099 mmol, 1.0 eq) and 1,2,3-triazole derivative 6 (63 mg, 0.1 mmol, 1.0 eq) in accordance with the general procedure. The reaction was performed at 80 °C and stopped (TLC, n-hexane/EtOAc3:7) after 8 days. Purification of the crude product (73.3 mg) by trituration with Et_2O afforded pure pyrrolidinium salt derivative **8b** (56 mg, 77% yield), as a very hygroscopic white solid; ^{1}H NMR (250.13 MHz, $CDCl_3$) δ = 7.74-7.51 (m, 3H, 2 × Ar-*H*, C*H*-triazole), 7.40 (m, 2H, 2 × Ar-*H*), 7.31 (m, 2H, 2 × Ar-*H*), 7.28-7.13 (m, 3H, 2 × Ar-*H*), 4.81, 4.45 (AB system, 2H, J_{AB} = 16.6 Hz, CH_2NSO$_2$), 4.20 (bt, 2H, J_{vic} = 6.4 Hz, CH_2N), 3.80 (d, 1H, J_{vic} = 10.2 Hz, C*H*NSO$_2$), 3.75-3.46 (m, 6H, 3 × CH_2N$^+$), 3.08 (s, 3H, CH_3N), 2.30 (m, 1H, C*H*Me$_2$), 2.25-1.95 (m, 4H, CH_2CH_2), 1.70-1.45 (m, 4H, CH_2CH$_2$N$^+$, CH_2CH$_2$N), 1.40-1.10 (m, 4H, *CH*$_2$*CH*$_2$), 1.04 (s, 9H, C*Me*$_3$), 0.74 (d, 3H, J_{vic} = 5.5 Hz, CH*Me*$_2$), 0.58 (d, 3H, J_{vic} = 6.4 Hz, CH*Me*$_2$); ^{13}C NMR (62.9 MHz, $CDCl_3$) δ = 169.3 (C=O), 145.6, 145.7 (*C*-triazole), 145.5 (Ar-*C*-SO$_2$, *C*-triazole), 139.0, 138.1 (2 × Ar-*C*), 128.9-127.1 (Ar-*C*H), 124.3 (*C*H-triazole), 81.9 (Me$_3$*C*O), 66.6 (*C*HNSO$_2$), 64.3 (2 × *C*H$_2$N$^+$), 63.7 (*C*H$_2$N$^+$), 49.8 (*C*H$_2$N), 48.5 (*C*H$_3$N), 40.3 (*C*H$_2$NSO$_2$), 29.5 (*C*H$_2$CH$_2$N$^+$), 23.5 (*C*H$_2$CH$_2$N), 28.8 (*CH*Me$_2$), 27.6 (*Me*$_3$C), 25.5, 25.3 (*C*H$_2$CH$_2$), 21.5 (*C*H$_2$CH$_2$), 19.7, 19.9 (CH*Me*$_2$). Anal. calcd for $C_{35}H_{52}BrN_5O_4S$: C 58.48, H 7.29, found: C 58.47, H, 7.27.

Piperidinium salt *tert*-butyl ester (8c). The title compound was prepared in dry MeCN (3.0 mL) from *N*-methyl-piperidine (**7b**) (9.80 mg, 0.099 mmol, 1.0 eq) and 1,2,3-triazole derivative **6** (62.6 mg, 0.099 mmol, 1.0 eq) in accordance with the general procedure. The reaction was performed at 80 °C and stopped (TLC, n-hexane/EtOAc 3:7) after 10 days. Purification of the crude product (74.6 mg) by trituration with Et_2O afforded pure piperidinium salt derivative **8c** (56.7 mg, 78% yield) as a very hygroscopic white solid; ^{1}H NMR (250.13 MHz, $CDCl_3$) δ = 7.73-7.50 (m, 3H, 2 × Ar-*H*, C*H*-triazole), 7.38 (m, 2H, 2 × Ar-H), 7.32 (m, 2H, 2 × Ar-H), 7.29-7.24 (m, 3H, 3 × Ar-H), 4.80, 4.44 (AB system, 2H, J_{AB} 16.7 Hz, CH_2NSO$_2$), 4.18 (bt, 2H, J_{vic} = 6.8 Hz, CH_2N), 3.79 (d, 1H, J_{vic} = 10.3 Hz, C*H*NSO$_2$), 3.54-3.33 (m, 6H, 3 × CH_2N$^+$), 3.10 (s, 3H, CH_3N), 2.10 (m, 1H, *CH*Me$_2$), 1.57-1.45 (m, 10H, CH_2CH$_2$N, CH_2CH$_2$N$^+$, CH_2CH_2CH_2), 1.41-1.10 (m, 4H, CH_2CH_2), 1.03 (s, 9H, *Me*$_3$C), 0.72 (d, 3H, J_{vic} = 6.6 Hz, *Me*$_2$CH), 0.52 (d, 3H, J_{vic} = 6.5 Hz, *Me*$_2$CH); ^{13}C NMR (62.9 MHz, $CDCl_3$) δ = 169.3 (C=O), 145.6, 145.4 (Ar-*C*-SO$_2$, *C*-triazole), 139.0, 138.1 (2 × Ar-*C*), 128.9-127.1 (Ar-*C*H), 124.3 (*C*H-triazole), 81.9 (Me$_3$*C*O), 66.6 (*C*HNSO$_2$), 62.9 (CH$_2$*CH*$_2$N$^+$), 60.7 (2×CH$_2$N$^+$), 49.8 (*C*H$_2$N), 47.9 (*C*H$_3$N), 40.3 (*C*H$_2$NSO$_2$), 29.5 (*C*H$_2$CH$_2$N$^+$) 21.5 (*C*H$_2$CH$_2$N), 28.8 (*CH*Me$_2$), 27.6 (*Me*$_3$C), 25.5, 25.3

(CH_2CH_2), 20.6, 20.0 ($CH_2CH_2CH_2$), 19.5, 18.9 (CH*Me*$_2$); Anal. calcd for $C_{36}H_{54}BrN_5O_4S$: C 59.00, H 7.43, found: C 58.88, H 7.44.

DABCO salt *tert*-butyl ester (8d). The title compound was prepared in dry EtOAc (0.4 mL) from 1,4-diazabicyclo[2.2.2]octane (DABCO, **7d**) (10.6 mg, 0.095 mmol, 1.0 eq) and 1,2,3-triazole derivative **6** (60.3 mg, 0.095 mmol, 1.0 eq) in accordance with the general procedure. The reaction was performed at room temperature and stopped (TLC, n-hexane/EtOAc 3:7) after 3 days. Purification of the crude product (68 mg) by trituration with Et_2O afforded pure DABCO salt derivative **8d** (65 mg, 92% yield), as a very hygroscopic white solid; ^{1}H NMR (250.13 MHz, $CDCl_3$) δ = 7.72 (m, 2H, 2×Ar-*H*), 7.66 (s, 1H, C*H*-triazole), 7.53 (m, 2H, 2×Ar-*H*), 7.40 (m, 2H, 2×Ar-H), 7.34-7.24 (m, 3H, 3×Ar-H), 4.79, 4.45 (AB system, 2H, J_{AB} = 16.7 Hz, C*H*$_2$NSO$_2$), 4.18 (bt, 2H, *Jvic* = 6.6 Hz, CH$_2$N), 3.79 (d, 1H, *Jvic* = 10.3 Hz, C*H*NSO$_2$), 3.48 (m, 6H, 3×C*H*$_2$N$^+$), 3.31 (m, 2H, C*H*$_2$N$^+$), 3.08 (m, 6H, 3×C*H*$_2$N), 2.10 (m, 1H, Me$_2$*CH*), 1.75-1.49 (m, 4H, C*H*$_2$CH$_2$N, C*H*$_2$CH$_2$N$^+$), 1.28-1.08 (m, 4H, C*H*$_2$*CH*$_2$), 1.03 (s, 9H, *Me*$_3$C), 0.74 (d, 3H, *Jvic* = 6.6 Hz, *Me*$_2$CH), 0.57 (d, 3H, *Jvic* = 6.5 Hz, *Me*$_2$CH); ^{13}C NMR (62.9 MHz, $CDCl_3$) δ = 169.3 (C=O), 145.7, 145.4 (Ar-*C*-SO$_2$, *C*-triazolo), 139.0, 138.1 (2 × Ar-*C*), 129.0-127.1 (Ar-*C*H), 124.1 (*C*H-triazolo), 81.9 (Me$_3$*C*O), 66.6 (*CH*NSO$_2$), 63.9 (CH$_2$*CH*$_2$N$^+$), 52.2 (3 × CH$_2$N$^+$ dabco), 49.8 (*CH*$_2$N), 45.2 (3 × *C*H$_2$N dabco), 40.2 (*C*H$_2$NSO$_2$), 29.5 *(*CH$_2$CH$_2$N$^+$), 21.5 (CH$_2$CH$_2$N), 28.8 (*CH*Me$_2$), 27.6 (*Me*$_3$C), 25.4, 25.3 (CH$_2$CH$_2$), 19.8, 18.9 (CH*Me*$_2$); Anal. calcd for $C_{36}H_{53}BrN_6O_4S$: C 57.98, H 7.16, found: C 57.96, H 7.15%.

Preparation of thioester derivative (9). To a solution of 1,2,3-triazole derivative **6** (249 mg, 0.393 mmol) in dry DMF (10 mL) was added potassium thioacetate (135 mg, 1.18 mmol) and the reaction mixture was stirred at 120 °C. After 2.5 h the solution was brown and TLC analysis (n-hexane/EtOAc 6:4) showed one product having the same R_f (0.33) of the starting material **6**. The solvent was evaporated under reduced pressure and the residue was partitioned between H_2O (20 mL) and CH_2Cl_2 (20 mL). The phases were separated, the organic layer was washed with H_2O (2 × 20 ml) and dried, filtered and concentrated under reduced pressure. Purification of the residue (291 mg) by flash chromatography on silica gel (n-hexane/EtOAc 6:4) afforded pure thioester **9** (242 mg, 98% yield) as a red oil; R_f = 0.33 (n-hexane/EtOAc 6:4); ^{1}H NMR (250.13 MHz, CD_3CN) δ = 7.86 (m, 2H, 2 × Ar-*H*), 7.77 (m, 2H, 2 × Ar-*H*), 7.75 (s, 1H, C*H*-triazole), 7.66 (m, 2H, 2 × Ar-*H*), 7.53-7.42 (m, 3H, 2 × Ar-*H*), 4.87, 4.68 (AB system, 2H, J_{AB} = 16.5 Hz, C*H*$_2$NSO$_2$), 4.28 (t, 2H, *Jvic* = 7.1 Hz, C*H*$_2$N), 3.95 (d, 1H, *Jvic* = 10.4 Hz, C*H*NSO$_2$), 2.78 (t, 2H, *Jvic* = 7.1 Hz, C*H*$_2$S), 2.27 (s, 3H, *Me*COS), 2.26-2.13 (m, 1H, *CH*Me$_2$), 1.84-1.72 (m, 2H, C*H*$_2$CH$_2$N),1.51-1.40 (m, 2H, C*H*$_2$CH$_2$S), 1.35 [m, 2H, *CH*$_2$(CH$_2$)$_2$N], 1.23 (s, 9H, C*Me*$_3$), 1.15 [m, 2H, *CH*$_2$(CH$_2$)$_2$S], 0.89 (d, 3H, *Jvic* = 6.6 Hz, CH*Me*$_2$), 0.72 (d, 3H, *Jvic* = 6.6 Hz, CH*Me*$_2$); ^{13}C NMR (62.9 MHz, CD_3CN) δ = 196.4 (*COS*), 170.4 (C=O), 146.1 (*C*-triazole), 145.8 (Ar-*C*-SO$_2$), 140.0, 139.9 (2 × Ar-*C*), 130.1-128.1 (Ar-*C*H), 125.0 (*C*H-triazole), 82.8 (Me$_3$*C*O), 67.6 (*CH*NSO$_2$), 50.6 (*C*H$_2$N), 41.0 (*C*H$_2$NSO$_2$), 29.4 (*C*H$_2$S), 30.7 (*C*H$_2$CH$_2$N), 30.1 (*C*H$_2$CH$_2$S), 31.3 (*Me*COS), 29.6 (*CH*Me$_2$), 28.6 [CH$_2$(CH$_2$)$_2$N], 26.4 [CH$_2$(CH$_2$)$_2$S], 27.9 (C*Me*$_3$), 20.4, 19.4 (CH*Me*$_2$); Anal. calcd for $C_{32}H_{44}N_4O_5S_2$: C 61.12, H 7.05, found: C 61.09, H 7.03.

General procedure for the preparation of carboxylic acids 12a-d. The appropriate *tert*-butyl ester derivative (**8a-d**, 0.1 mmol) was dissolved in H_2O (5.0 mL), treated with commercial 48% aq. HBr (0.59 mL) and stirred at room temperature. After 8-12 h, TLC analysis ($CHCl_3$/MeOH 8:2, triple elution) revealed the complete disappearance of the starting material. The solution was co-evaporated with toluene (5 ×10 mL) under reduced pressure and the purification of crude product by trituration with Et_2O afforded pure carboxylic acids derivatives **12a-d**.

Deprotected imidazolium salt derivative (12a). Acid hydrolysis of **8a** (63 mg, 0.087 mmol) was performed according to the general procedure. The reaction was stopped after 8 h (TLC, $CHCl_3$/MeOH 8:2, triple elution) and the purification of crude product (32 mg) by trituration with Et_2O afforded pure carboxylic acid **12a** (52.8 mg, 92% yield), as a very hygroscopic white solid; R_f = 0.23 ($CHCl_3$/MeOH 8:2, triple elution); ^{1}H NMR (250.13 MHz, CD_3OD/D_2O) δ = 9.00 (s, 1H, Im-*H*$_2$), 8.40 (m, 1H, C*H*-triazole), 7.94-7.82 (m, 4H, 4 × Ar-*H*), 7.72-7.42 (m, 7H, 5 × Ar-*H*, Im-*H*$_4$, Im-*H*$_5$), 4.72, 5.00 (2bd, each 1H, J_{gem} = 17.5 Hz, C*H*$_2$NSO$_2$), 4.54 (bt, 2H, *Jvic* = 7.1 Hz, CH$_2$N), 4.21 (bt, 2H, *Jvic* = 7.2 Hz, CH$_2$N), 4.09 (d, 1H, *Jvic* = 10.3 Hz, C*H*NSO$_2$), 3.93 (s, 3H, C*H*$_3$N), 2.18 (m, 1H, C*H*Me$_2$), 1.96-1.87 (m, 4H, 2 × C*H*$_2$CH$_2$N), 1.44-1.36 (m, 4H, C*H*$_2$C*H*$_2$), 0.99 (d, 3H, *Jvic* = 6.6 Hz, CH*Me*$_2$), 0.80 (d, 3H, *Jvic* = 6.6 Hz, CH*Me*$_2$); ^{13}C NMR (62.9 MHz, CD_3OD/D_2O) δ = 173.4(C=O), 147.2 (Ar-*C*-SO$_2$, *C*-triazole), 140.2,138.9 (2 × Ar-*C*), 137.9 (Im-*C*$_2$), 130.2-128.3 (Ar-*C*H), 125.0, 125.0, 123.7 (*C*H-triazole, Im-*C*$_4$, Im-*C*$_5$), 67.4 (*CH*NSO$_2$), 52.9, 50.6 (2×CH$_2$N), 39.8 (*C*H$_2$NSO$_2$), 36.7 (*C*H$_3$N), 30.8, 30.6 (2×C*H*$_2$CH$_2$N), 29.9 (*CH*Me$_2$), 26.5, 26.4 (C*H*$_2$*CH*$_2$), 20.3, 19.6 (CH*Me*$_2$); Anal. calcd for $C_{30}H_{39}BrN_6O_4S$: C 54.62, H 5.96%, found: C 54.60, H 5.98.

Deprotected pyrrolidinium salt derivative (12b). Acid hydrolysis of **8b** (39.2 mg, 0.055 mmol) was performed according to the general procedure. The reaction was stopped after 8 h (TLC, $CHCl_3$/MeOH 8:2, triple elution) and the co-evaporated with toluene under reduced pressure afforded a syrup constituted (NMR) by pure carboxylic acids **12b** (34 mg, 94% yield), R_f = 0.33 ($CHCl_3$/MeOH 8:2, triple elution); ^{1}H NMR (250.13 MHz, CD_3OD) δ = 7.96-7.65 (m, 7H, 6 × Ar-*H*, *C*H-triazole), 7.49-7.38 (m, 3H, 2 × Ar-*H*), 5.05 (m, 2H, C*H*$_2$NSO$_2$), 3.91 (m, 1H, C*H*NSO$_2$),3.70-2.90 (m, 8H, CH$_2$N, 3 × C*H*$_2$N$^+$), 3.10 (s, 3H, C*H*$_3$N), 2.20-2.08 (m, 4H, C*H*$_2$C*H*$_2$), 2.05-1.63 (m, 5H, *CH*Me$_2$, C*H*$_2$CH$_2$N, C*H*$_2$CH$_2$N$^+$), 1.55-1.20 (m, 4H, C*H*$_2$C*H*$_2$), 0.91, 0.82 (2s, each 3H, *Me*$_2$CH); ^{13}C NMR (62.9 MHz, CD_3OD) δ = 173.0 (C=O), 145.5, 145.4 (Ar-*C*-SO$_2$, *C*-triazole), 138.9, 137.7 (2 × Ar-*C*), 128.7-126.8 (Ar-*C*H), 125.1 (*C*H-triazole), 66.2 (*CH*NSO$_2$), 64.0 (2 × *C*H$_2$N$^+$), 63.4 (*CH*$_2$N$^+$), 49.9 (*CH*$_2$N), 47.4 (*CH*$_3$N), 43.1 (*CH*$_2$NSO$_2$), 29.2 (*CH*$_2$CH$_2$N$^+$), 29.1 (*CH*Me$_2$), 25.2, 25.1 (*CH*$_2$*CH*$_2$), 23.5 (*CH*$_2$CH$_2$N), 21.1 (*CH*$_2$*CH*$_2$), 19.0, 18.2 (*Me*$_2$CH); Anal. calcd for $C_{31}H_{44}BrN_5O_4S$: C 56.19, H 6.69, found: C 56.17, H 6.67.

Deprotected piperidinium salt derivative (12c). Acid hydrolysis of **8c** (45 mg, 0.061 mmol) was performed according to the general procedure. The reaction was stopped after 48 h (TLC, $CHCl_3$/MeOH 8:2, triple elution) and the purification of crude product (47 mg) by trituration with Et_2O afforded pure carboxylic acids **12c** (38.6 mg, 93% yield) as a very hygroscopic white solid; R_f = 0.35 ($CHCl_3$/MeOH 8:2, triple elution); ^{1}H NMR (250.13 MHz, CD_3OD/D_2O) δ = 7.90 (m, 3H, 2 × Ar-*H*, *C*H-triazole), 7.81 (m, 2H, 2 × Ar-*H*), 7.70 (m, 2H, 2 × Ar-*H*), 7.51-7.45 (m, 3H, 3 × Ar-*H*), 4.82, 4.65 (AB system, 2H, J_{AB} = 16.1 Hz, C*H*$_2$NSO$_2$), 4.39 (m, 2H, CH$_2$N), 4.09 (bd, 1H, *Jvic* = 10.1 Hz, C*H*NSO$_2$), 3.48-3.20 (m, 6H, 3 × C*H*$_2$N$^+$), 3.32 (s, 3H, C*H*$_3$N), 2.24 (m, 1H, *CH*Me$_2$), 2.10-1.81 (6H, m, 3 × C*H*$_2$CH$_2$N$^+$), 1.78-1.55 (m, 4H, C*H*$_2$CH$_2$N, CH$_2$C*H*$_2$CH$_2$), 1.42-1.23 (m, 4H, C*H*$_2$C*H*$_2$), 0.95, 0.79 (2s, each 3H, CH*Me*$_2$); ^{13}C NMR (62.9 MHz, CD_3OD) δ = 173.3 (C=O), 146.9, 146.8 (Ar-*C*-SO$_2$, *C*-triazole), 140.4, 139.4 (2 × Ar-*C*), 130.2-128.3 (Ar-*C*H), 126.2 (*C*H-triazole), 67.6 (*CH*NSO$_2$), 64.9 (CH$_2$*CH*$_2$N$^+$), 62.2 (2 × *C*H$_2$N$^+$), 51.0 (*C*H$_2$N), 47.7 (*C*H$_3$N), 41.1 (*C*H$_2$NSO$_2$), 30.8 (*C*H$_2$CH$_2$N$^+$) 29.7 (*CH*Me$_2$), 26.7, 26.6 (*C*H$_2$CH$_2$), 20.9 (*C*H$_2$CH$_2$N$^+$), 22.5, 22.1 (CH$_2$CH$_2$CH$_2$, *C*H$_2$CH$_2$N), 20.3, 19.6 (CH*Me*$_2$); Anal. calcd for $C_{32}H_{46}BrN_5O_4S$: C 56.80, H 6.85%, found: C 56.78, H 6.83.

Deprotected DABCO salt derivative (12d). Acid hydrolysis of **8d** (51.3 mg, 0.069 mmol) was performed according to the general procedure. The reaction was stopped after 48 h (TLC, $CHCl_3$/MeOH 7:3) and the purification of crude product (52.8 mg) by trituration with Et_2O afforded pure carboxylic acids **12d** (46.9 mg, 99% yield) as a very hygroscopic white solid; R_f = 0.22 ($CHCl_3$/MeOH 7:3); ^{1}H NMR (250.13 MHz, CD_3OD/D_2O) δ = 7.89 (m, 3H, 2 × Ar-*H*, *C*H-triazole), 7.78 (m, 2H, 2 × Ar-*H*), 7.66 (m, 2H, 2 × Ar-*H*), 7.51-7.38 (m, 3H, 3 × Ar-*H*), 4.87, 4.61 (AB system, 2H, J_{AB} = 15.7 Hz, C*H*$_2$NSO$_2$), 4.38 (bt, 2H, *Jvic* = 6.0 Hz, C*H*$_2$N), 4.03 (d, 1H, *Jvic* = 10.1 Hz, C*H*NSO$_2$), 3.62-3.10 (m, 14H, 4 × C*H*$_2$N$^+$, 3 × C*H*$_2$N), 2.22 (m, 1H, *CH*Me$_2$), 1.90 (m, 2H, C*H*$_2$CH$_2$N$^+$), 1.76 (m, 2H, C*H*$_2$CH$_2$N), 1.45-1.22 (m, 4H, C*H*$_2$C*H*$_2$), 0.96 (d, 3H, *Jvic* = 6.5 Hz, CH*Me*$_2$), 0.78 (d, 3H, *Jvic* = 6.3 Hz, CH*Me*$_2$); ^{13}C NMR (62.9 MHz, CD_3OD/D_2O) δ =173.2 (C=O), 146.8, 146.3 (Ar-*C*-SO$_2$, *C*-triazole), 140.1, 138.9 (2 × Ar-*C*), 129.9-128.1 (Ar-*C*H), 125.8 (*C*H-triazole), 67.4 (*CH*NSO$_2$), 65.4, 64.6 (4 × CH$_2$N$^+$), 52.9 (3 × *C*H$_2$N), 50.8 (*C*H$_2$N), 41.0 (*C*H$_2$NSO$_2$), 30.5 (*C*H$_2$CH$_2$N$^+$), 29.5 (*CH*Me$_2$), 26.4, 26.2 (*C*H$_2$CH$_2$), 22.4 (*C*H$_2$CH$_2$N), 20.3,

19.6 (CH*Me*$_2$); Anal. calcd for $C_{32}H_{45}BrN_6O_4S$: C 55.73, H 6.58, found: C 55.70, H 6.55.

Preparation of deprotected thiol derivative (11). The *tert*-butyl ester **9** (30 mg, 0.048 mmol) was dissolved in CH_2Cl_2 (1.0 mL), treated with CF_3COOH (0.18 mL) and stirred at 0°C for 1 h and then at room temperature. After 8 h, TLC analysis (n-hexane/EtOAc 3:7) revealed the complete disappearance of the starting material and the solution was coevaporated with toluene (5 × 10 mL) under diminished pressure. The purification of crude product by chromatography over silica gel (n-hexane/EtOAc 3:7) afforded a crude product constituted exclusively (NMR) by carboxylic acid **10** (27 mg, 98% yield) as a very viscous yellow-brown oil; R_f = 0.21 (n-hexane/EtOAc 3:7); ^{1}H NMR (250.13 MHz, $CDCl_3$) δ = 10.8 (bs, 1H, OH), 7.84 (m, 2H, 2 × Ar-*H*), 7.75 (m, 2H, 2 × Ar-*H*), 7.72 (s, 1H, C*H*-triazole), 7.64 (m, 2H, 2 × Ar-H), 7.53-7.41 (m, 3H, 3 × Ar-H), 4.89, 4.69 (AB system, 2H, J_{AB} = 16.3 Hz, CH_2NSO$_2$), 4.31 (t, 2H, J_{vic} = 7.1 Hz, CH_2N), 3.92 (d, 1H, J_{vic} = 10.4 Hz, C*H*NSO$_2$), 2.76 (t, 2H, J_{vic} = 7.1 Hz, CH_2S), 2.25 (s, 3H, *Me*COS), 2.20-2.11 (m, 1H, *CH*Me$_2$), 1.82-1.70 (m, 2H, CH_2CH$_2$N),1.49-1.40 (m, 2H, CH_2CH$_2$S), 1.37 [m, 2H, *CH*$_2$(CH$_2$)$_2$N], 1.15 [m, 2H, *CH*$_2$(CH$_2$)$_2$S], 0.92 (d, 3H, J_{vic} = 6.7 Hz, CH*Me*$_2$), 0.75 (d, 3H, J_{vic} = 6.7 Hz, CH*Me*$_2$); ^{13}C NMR (62.9 MHz, $CDCl_3$) δ = 196.4 (*COS*), 170.4 (C=O), 146.1 (*C*-triazole), 145.8 (Ar-*C*-SO$_2$), 140.0, 139.9 (2 × Ar-*C*), 130.1-128.1 (Ar-*C*H), 125.0 (*C*H-triazole), 67.6 (*CH*NSO$_2$), 50.6 (*C*H$_2$N), 41.0 (*C*H$_2$NSO$_2$), 29.4 (*C*H$_2$S), 30.7 (*C*H$_2$CH$_2$N), 30.1 (*C*H$_2$CH$_2$S), 31.3 (*Me*COS), 29.6 (*CH*Me$_2$), 28.6 [*C*H$_2$(CH$_2$)$_2$N], 26.4 [*C*H$_2$(CH$_2$)$_2$S], 20.4, 19.4 (CH*Me*$_2$).

A solution of the crude thioester derivative **10** (27 mg, 0.047 mmol) in MeOH (0.77 mL) was treated with NH_3-MeOH 7N (0.77 mL) and the solution was stirred at room temperature until TLC analysis (n-hexane/EtOAc 3:7) shows the disappearance of the starting material (R_f = 0.24) and the formation of a single product at R_f = 0.01. After 4 h the solution was neutralized with resin acid (Amberlite® IR120 H), stirred at room temperature (5 min), filtered and the resin was washed with MeOH. The collected organic phases were concentrated under reduced pressure and the trituration of crude product (25 mg) with Et_2O afforded pure thiol derivative **11** (22.1 mg, 89% yield) as a hygroscopic white solid; R_f = 0.01 (n-hexane/EtOAc 3:7); ^{1}H NMR (250.13 MHz, $CDCl_3$) δ = 9.29 (bs, 1H, OH), 7.83 (m, 1H, 2 × Ar-*H*, C*H*-triazole), 7.74 (m, 2H, Ar-*H*), 7.52 (m, 2H, Ar-*H*), 7.47-7.37 (m, 3H, Ar-*H*), 5.03, 4.85 (AB system, 2H, J_{AB} = 16.3 Hz, CH_2NSO$_2$), 4.72 (bt, 2H, CH_2N), 4.11 (d, 1H, J_{vic} = 10.1 Hz, C*H*NSO$_2$), 2.61 (t, 2H, J_{vic} = 7.1 Hz, CH_2SH), 2.15 (m, 1H, *CH*Me$_2$), 1.85 (m, 2H, CH_2CH$_2$N), 1.61 (m, 2H, CH_2CH$_2$SH), 1.40 [m, 2H, *CH*$_2$(CH$_2$)$_2$N], 1.18 [m, 2H, *CH*$_2$(CH$_2$)$_2$SH], 0.87 (d, 3H, J_{vic} = 6.4 Hz, CH*Me*$_2$), 0.69 (d, 3H, J_{vic} = 6.4 Hz, CH*Me*$_2$); ^{13}C NMR (62.9 MHz, $CDCl_3$) δ = 171.7 (C=O), 146.6 (*C*-triazole), 145.8 (Ar-*C*-SO$_2$), 139.8, 138.3 (2 × Ar-*C*), 129.6-127.9 (Ar-*C*H), 125.0 (*C*H-triazole), 67.0 (*CH*NSO$_2$), 51.2 (*C*H$_2$N), 40.8 (*C*H$_2$NSO$_2$), 39.3 (*C*H$_2$SH), 30.6 (*C*H$_2$CH$_2$N), 29.5 (*C*H$_2$CH$_2$SH), 29.1 (*CH*Me$_2$), 28.3 [*C*H$_2$(CH$_2$)$_2$N], 26.6 [*C*H$_2$(CH$_2$)$_2$S], 20.3, 20.0 (CH*Me*$_2$); Anal. calcd for $C_{26}H_{34}N_4O_4S$: C 58.84, H 6.46, found: C 58.83, H 6.44.

Preparation of gold nanoparticles Au-S (13). To a solution of thiol derivative **11** (10.0 mg, 0.019 mmol) in $CHCl_3$ (2.5 mL) was added ALIQUAT 336 (1.11 mg, 0.0027 mmol) and the mixture was stirred vigorously at room temperature. After 5 min was added an aqueous solution of $HAuCl_4$ 2.5×10^{-3} M (0.68 ml, 1.71×10^{-3} mmol) and the mixture was stirred until the aqueous layer became transparent. The dark-yellow organic phase was separated from the aqueous solution and transferred in a bottom flask (10 mL) with a magnetic bar. A fresh aqueous solution of excess of $NaBH_4$ 0.1 M (200 µl) was added to the organic layer under vigorous stirring. The color of solution immediately changes to dark-red/brown and the reaction mixture was stirred at room temperature. After 3 h the organic layer was separated and purified by dialysis using dialysis tubing (Sigma-Aldrich) 14 kDa previously washed and activated (see materials and methods). The solvent was evaporated under reduced pressure and the **Au-S (13)** (14.1 mg) was characterized by UV-Vis spectroscopy, NMR and TEM.

Preparation of gold nanoparticles Au-IL (14). To a solution of the imidazolium salt **12a** (19.5 mg, 0.029 mmol) in a 0.1:1 MeO-H_2O (2.2 mL) was added an aqueous solution of $HAuCl_4$ 2.5 × 10^{-3} M (0.1 ml, 2.5 × 10^{-4} mmol) and the solution was stirred vigorously at room temperature (5 min). A fresh aqueous solution of $NaBH_4$ 0.1 M (200 µl) was added drop by drop (1 h) to the mixture under vigorous stirring and the color of the solution slowly change from yellow to dark red-violet. The reaction mixture was stirred at room temperature (3 h) and the crude gold nanoparticles **Au-IL (14**) were purified by simple centrifugal filtering (4000 rpm for 40 min) using the Millipore filters Amicon Ultra-4. The residue in the AMICON filter was dispersed in milliQ water (3 mL) and centrifuged again, repeating this process (2-3 times) until the TLC analysis ($CHCl_3$/MeOH 8:2, triple elution) showed the disappearance of the excess of the starting ligand **12a**. The gold nanoparticles dispersed in water were characterized by UV-Vis spectroscopy and TEM. The gold nanoparticle **Au-IL (14)** were water soluble and stable for 2 months in solution (see Supporting Information, Figure S3).

MMP inhibition assays. Recombinant human pro-MMP-2 and pro-MMP-9 were purchased from Calbiochem (Merck-Millipore). Pro-MMP-12 was purchased by R&D Systems. Proenzymes were activated immediately prior to use with *p*-aminophenylmercuric acetate (2 mM APMA for 1 h at 37 °C for MMP-2 and 1 mM APMA for 1 h at 37 °C for MMP-9). Pro-MMP-12 was auto activated by incubating in Fluorometric Assay Buffer (FAB: Tris 50 mM, pH 7.5, NaCl 150 mM, $CaCl_2$ 10 mM, Brij-35 0.05%, and DMSO 1%) for 30 h at 37 °C. For assay measurements, the inhibitor stock solutions (DMSO, 10 mM) were further diluted in FAB. Activated enzyme (final concentrations of 0.56 nM for MMP-2, 1.3 nM for MMP-9, 2.3 nM for MMP-12) and inhibitor solutions were incubated in the assay buffer for 3 h at 25 °C. After the addition of 200 µM solution of the fluorogenic substrate Mca-Lys-Pro-Leu-Gly-Leu-Dap(Dnp)-Ala-Arg-NH_2 (Bachem) for all the enzymes in DMSO (final concentration of 2 µM for all enzymes), the hydrolysis was monitored every 10 s for 15 min, recording the increase in fluorescence (λ_{ex} = 325 nm, λ_{em} = 400 nm) with a Molecular Devices SpectraMax Gemini XPS plate reader. The assays were performed in duplicate in a total volume of 200 µL per well in 96-well microtiter plates (Corning black, NBS). Control wells lack inhibitor. The MMP inhibition activity was expressed in relative fluorescent units (RFU). Percent of inhibition was calculated from control reactions without the inhibitor. IC_{50} was determined using the formula v_i/v_0 = 1/(1 + [I]/IC50), where v_i is the initial velocity of substrate cleavage in the presence of the inhibitor at concentration [I] and v_o is the initial velocity in the absence of the inhibitor. Results were analyzed using SoftMax Pro software and Prism Software version 5.0 (GraphPad Software, Inc., La Jolla, C.A.).

Preparation of dendritic cells. Peripheral blood mononuclear cells (PBMC) were obtained after Ficoll-Hypaque density centrifugation of blood samples derived from healthy donors (institutional informed consent signed at the time of donation). Monocytes were isolated from PBMC using the anti-CD14 mAb (MEM18, IgG1, Exbio, Prague, CZ) and EasySep custom Kit (Stemcell Technologies) according to manufacturer's instructions, with recovery of >97% CD14 positive cells.[38] Dendritic cells (DC) were obtained by culturing monocytes in RPMI 1640 medium with 10% bovine serum, 20 ng/mL GMCSF and 20 ng/mL IL4 for 7 days.[39] DC were about 40-50% CD1a$^+$, as evaluated by immunofluorescence (not shown).

FACS analysis and confocal microscopy. FACS analysis was performed upon addition of **EDV2** compound, at 10 to 1 µM concentrations and for 30 min at 37 °C to iDC or mDC. Unrelated FITC-conjugated immunoglobulins (Ig) were used as negative controls. Samples were then washed and analyzed on a CyAn ADP Analyzer (Beckman Coulter, Milano, Italy). Results are shown as mean fluorescence intensity (MFI, arbitrary units, a.u.) vs number of cells or as MFI ratio (MFI sample/MFI negative control). In some experiments, DC were treated with 10 µM **EDV2** and 1 µM Syto62 for 1 h at 37 °C, washed, seeded onto glass slides and analyzed by confocal microscopy under a FV500 (Olympus Europe) with PlanApo 40x NA1.00 oil objectives and data analyzed with FluoView 4.3b

software (Olympus). Images were then taken in sequence mode and shown in pseudocolor.

Matrigel invasion assay. DC ($5x10^5$) were seeded in the inset of 12w transwell chambers (Costar Corning, NY, USA, pore size 3 μm), coated for 1 h at RT with Matrigel (Corning, 0.5 mg/mL), in the absence or presence of compound **1** or **12a** at 10 μM concentration, and incubated overnight at 37 °C in a CO_2 humidified incubator. Cells were recovered from the lower chamber and counted at the MACS Quant Analyzer 10 (Miltenyi Biotech GmbH, Bergisch Gladbach, Germany).

Statistical analysis. Data are presented as mean ± SD. Statistical analysis was performed using two-tails student's t test. The cut-off value of significance is indicated in each figure legend.

TEM analysis. mDC exposed to AuNPs **Au-S (13)** and **Au-IL (14)**, at 2.5 μM concentration, overnight, were washed and treated with cacodylate buffer 0.1 M (pH 7.5) for 5 min, centrifuged at 5,000 rpm for 5 min, prefixed in Karnovsky's solution (1% paraformaldehyde, 2% glutaraldehyde, 2 mM calcium chloride, 0.1 M cacodylate buffer, pH 7.5) for 2 h at 4 °C, and finally washed with cacodylate buffer. Postfixing was carried out in 1% osmium tetroxide in cacodylate buffer for 1 h. After dehydration with 70% to 100% alcohol, the cells were embedded in Poly/Bed 812 resin (Polysciences, Inc., Warrington, PA) and polymerized. Ultrathin sections were stained by a double contrast method with a solution of uranyl acetate in 50% ethanol followed by 0.4% aqueous lead citrate and examined by TEM. To evaluate the size of gold nanoparticles, 5 μL of each sample solution were adsorbed for 1 min onto carbon coated 300-mesh Copper grids. All air-dried specimens were examined with TEM. TEM was performed with a Zeiss LEO 900 Electron Microscope (Zeiss, Stuttgart, Germany) operating at 80 kV. Images flattening and analysis of size was performed by ImageJ software and Origin Pro8.

Acknowledgements

The present work has been partially funded by PRA_2015_0015 and PRA_2017_51 (University of Pisa). The author thank Maria Gerarda Cianci and Martina Bragazzi (University of Pisa) for the contribution to the synthesis of compounds **12b-c**, Francesca Tosetti (Policlinico San Martino, Genoa) for preparation of TEM images and helpful discussion and Serena Varesano (Policlinico San Martino, Genoa) for the preparation of monocytes and DC.

Keywords: bioactive Ionic Liquids • Gold Nanoparticles • MMP-12 inhibitors • metalloproteins.

References:

[1] G. Murphy, H. Nagase, *Mol. Aspects Med.* **2008**, *29*, 290-308.
[2] R. E. Vandenbroucke, C. Libert, *Nat. Rev. Drug Discov.* **2014**, *13*, 904-927.
[3] V. Lagente, C. Le Quement, E. Boichot, *Expert Opin. Ther. Targets* **2009**, *13*, 287-295.
[4] W. Li, J. Li, Y. Wu, F. Rancati, S. Vallese, L. Raveglia, J. Wu, R. Hotchandani, N. Fuller, K. Cunningham, P. Morgan, S. Fish, R. Krykbaev, X. Xu, S. Tam, S. J. Goldman, W. Abraham, C. Williams, J. Sypek, T. S. Mansour. *J. Med. Chem.* **2009**, *52*, 5408-5419.
[5] A. C. Newby, *Vascul. Pharmacol.* **2012**, *56*, 232-244.
[6] E. Nuti, D. Cuffaro, F. D'Andrea, L. Rosalia, L. Tepshi, M. Fabbi, G. Carbotti, S. Ferrini, S. Santamaria, C. Camodeca, L. Ciccone, E. Orlandini, S. Nencetti, E. A. Stura, V. Dive, A. Rossello, *ChemMedChem* **2016**, *11*, 1626-1637.
[7] P. Wasserscheid, T. Welton, in "Ionic Liquids in Synthesis", 2nd ed; Wiley-VCH: Weinheim, Germany, 2008.
[8] C. Antoni, L. Vera, L. Devel, M. P. Catalani, B. Czarny, E. Cassar-Lajeunesse, E. Nuti, A. Rossello, V. Dive, E. A. Stura, *J. Struct. Biol.* **2013**, *182*, 246-254.
[9] E. Nuti, L. Rosalia, D. Cuffaro, C. Camodeca, C. Giacomelli, E. Da Pozzo, T. Tuccinardi, B. Costa, C. Antoni, L. Vera, L. Ciccone, E. Orlandini, S. Nencetti, V. Dive, C. Martini, E. A. Stura, A. Rossello, *ACS Med. Chem. Lett.* **2017**, *8*, 293-298.
[10] R. Ferraz, L. C. Branco, C. Prudêncio, J. P. Noronha, Z. Petrovski, *ChemMedChem*. **2011**, *6*, 975-985.
[11] K. S. Egorova, E. G. Gordeev, V. P. Ananikov, *Chem. Rev.* **2017**, *117*, 7132−7189.
[12] C. Janiak, *Zeitschrift für Naturforschung B* **2013**, *68*, 1059-1089.
[13] E. J. W. Verwey, *J. Phys. Chem.* **1947**, *51*, 631-636.
[14] K. Ghandi, A. D. Findlater, Z. Mahimwalla, C. S, MacNeil, E. Awoonor-Williams, F. Zahariev, M. S. Gordon *Nanoscale*, **2015**, *7*, 11545-11551.
[15] M. Antonietti, D. Kuang, B. Smarsly, Y. Zhou, *Angew. Chem. Int. Ed.* **2004**, *43*, 4988-4992.
[16] E. Husanu, C. Chiappe, A. Bernardini, V. Cappello, M. Gemmi, *Colloids and Surfaces A* **2018**, *538*, 506-512
[17] E. Husanu, V. Cappello, C. S. Pomelli, J. David, M. Gemmi, C. Chiappe, *RSC Advances* **2017**, *7*, 1154-1160.
[18] W. Huang, S. Chen, Y. Liu, H. Fu, G. Wu, *Nanotechnology* **2011**, *22*, 025602-025609.
[19] T. Bordenave, M. Helle, F. Beau, D. Georgiadis, L. Tepshi, M. Bernes, Y. Ye, L. Levenez, E. Poquet, H. Nozach, M. Razavian, J. Toczek, E. A. Stura, V. Dive, M. M. Sadeghi, L. Devel, *Bioconjug. Chem.* **2016**, *27*, 2407-2417.
[20] N.H. Lim, E. Meinjohanns, G. Bou-Gharios, L. L. Gompels, E. Nuti, A. Rossello, L. Devel, V. Dive, M. Meldal, H. Nagase, *Arthritis Rheumatol*. **2014**, *66*, 589-98.
[21] a) V. Hugenberg, S. Wagner, K. Kopka, M. Schäfers, R. C. Schuit, A. D. Windhorst, S. Hermann, *J. Med. Chem.* **2017**, *60*, 307-321; b) V. Butsch, F. Börgel, F. Galla, K. Schwegmann, S. Hermann, M. Schäfers, B. Riemann, B. Wünsch, S. Wagner, *J. Med. Chem*. **2018**, *61*, 4115-4134.
[22] F. Casalini, L. Fugazza, G. Esposito, C. Cabella, C. Brioschi, A. Cordaro, L. D'Angeli, A. Bartoli, A.M. Filannino, C. V. Gringeri, D. L. Longo, V. Muzio, E. Nuti, E. Orlandini, G. Figlia, A. Quattrini, L. Tei, G. Digilio, A. Rossello, A. Maiocchi, *J. Med. Chem.* **2013**, *56*, 2676-89.
[23] M.-C. Daniel, D. Astruc, *Chem. Rev.* **2004**, *104*, 293-346.
[24] C. Romuald, E. Busseron and F. Coutrot, *J. Org. Chem.* **2010**, *75*, 6516-6531.
[25] J. A. F. Joosten, N. T. H. Tholen, F. Ait El Maate, A. J. Brouwer, G. W. van Esse, D. T. S. Rijkers, R. M. J. Liskamp and R. J. Pieters, *Eur. J. Org. Chem.* **2005**, *15*, 3182-3185.
[26] J. D. Diot, I. Garcia Moreno, G. Twigg, C. Ortiz Mellet, K. Haupt, T. D. Butters, J. Kovensky and S. G. Gouin, *J. Org. Chem.* **2011**, *76*, 7757-7768.
[27] M. Brust, M. Walker, D. Bethell, D. J. Schiffrin, R. Whyman, *J. Chem. Soc., Chem. Commun.* **1994**, 801-802.
[28] J. Huang , Y. Han, in "*Recent Progress in Colloid and Surface Chemistry with Biological Applications*", Edited by C. Wang and R. M. Leblanc, **2016**, *12*, 213-243.
[29] E. C. Dreaden, S. C. Mwakwari, Q. H. SodjiAdegboyega, K. Oyelere, M.A. El-Sayed, *Bioconjugate Chem.,* **2009**, *20*, 2247-2253.
[30] K. G. Thomas, P. V. Kamat, *Acc. Chem. Res.,* **2003**, *36*, 888-898.
[31] A. Triolo, O. Russina, B Fazio, G. B. Appetecchi, M Carewska, S. Passerini, *J. Chem.Phys.,* **2009**, *130*, 164521-164526.
[32] U. Neumann, H. Kubota, K. Frei, V. Ganu, D. Leppert, *Anal. Biochem.* **2004**, *328*, 166-173.
[33] K. Kis-Toth, I. Bacskai, P. Gogolak, A. Mazlo, I. Szatmari, E. Rajnavolgyi, *Immunobiology*, **2013**, *218*, 1361-1369.
[34] a) D. J. Marchant, C. L. Bellac, T. J. Moraes, S. J. Wadsworth, A. Dufour, G. S. Butler, L. M. Bilawchuk, R. G. Hendry, A. G. Robertson, C. T. Cheung, J. Ng, L. Ang, Z. Luo, K. Heilbron, M. J. Norris, W. Duan, T. Bucyk, A. Karpov, L. Devel, D. Georgiadis, R. G. Hegele, H. Luo, D. J. Granville, V. Dive, B. M. McManus, C. M. Overall, *Nat. Med.* **2014**, *20*, 493-502; b) R. K. Koppisetti, Y. G. Fulcher, A. Jurkevich, S. H. Prior, J. Xu, M. Lenoir, M. Overduin, S. R. Van Doren, *Nat. Commun.* **2014**, *5*, 5552.

[35] a) B. D. Chithrani, W. C. Chan, *Nano Lett.* **2007**, *7*, 1542-1550; b) S. H. Wang, C. W. Lee, A. Chiou, P. K. Wei, *J. Nanobiotechnology* **2010**, *8*, 33.

[36] a) F. Tosetti, R. Venè, C. Camodeca, E. Nuti, A. Rossello, C. D'Arrigo, D. Galante, N. Ferrari, A. Poggi, M. R. Zocchi. *Oncoimmunology* **2018**, *7*, e1421889; b) C. Camodeca, E. Nuti, F. Tosetti, A. Poggi, C. D'Arrigo, M. R. Zocchi, A. Rossello, *ChemMedChem.* **2018**, *13*, 2119-2131.

[37] D. D. Perrin, W. L. F. Armarengo and D. R. Perrin, Purification of Laboratory Chemicals, 2nd ed., Pergamon, Oxford, **1980**.

[38] A. Musso, S. Catellani, P. Canevali, S. Tavella, R. Venè, S. Boero, I. Pierri, M. Gobbi, A. Kunkl, J. L. Ravetti, M. R. Zocchi, A. Poggi, *Haematologica*. **2014**, *99*, 131-139.

[39] S. Sozzani, F. Sallusto, W. Luini, D. Zhou, L. Piemonti, P. Allavena, J. Van Damme, S. Valitutti, A. Lanzavecchia, A. Mantovani, *J. Immunol.* **1995**, *155*, 3292-3295.

Entry for the Table of Contents

Ionic Liquids in Drug Synthesis: Ionic liquid-based MMP-12 inhibitors have been synthesized for the first time and used to prepare electrostatically stabilized MMP inhibitors-coated gold nanoparticles (AuNPs). These ionic AuNPs were water soluble, stable, able to selectively bind MMP-12 in vitro and have been used as an innovative bioimaging probe to stain MMP-12 in monocyte-derived dendritic cells.